Journal of Molecular Catalysis A: Chemical 373 (2013) 25–29

Contents lists available at SciVerse ScienceDirect

Journal of Molecular Catalysis A: Chemical

journal homepage: www.elsevier.com/locate/molcata

Magnetic nanoparticle supported polyoxometalate: An efficient and reusable catalyst for solvent-free synthesis of α-aminophosphonates

H. Hamadi[a], M. Kooti[a,*], M. Afshari[a], Z. Ghiasifar[b], N. Adibpour[c]

[a] Department of Chemistry, College of Science, Shahid Chamran University, Ahvaz 61357-43169, Iran
[b] Department of Chemistry, Science and Research Khouzestan Branch, Islamic Azad University, Ahvaz, Iran
[c] Department of Pharmacology and Toxicology, School of Pharmacy, Ahvaz Jundishpur University of Medical Sciences, Ahvaz, Iran

ARTICLE INFO

Article history:
Received 21 June 2012
Received in revised form 7 January 2013
Accepted 17 February 2013
Available online 28 February 2013

Keywords:
Cobalt ferrite
α-Aminophosphonates
Magnetic nanoparticles
Surface functionalization
Phosphotungstic acid

ABSTRACT

A new magnetically separable catalyst consisting of phosphotungstic acid (PTA) supported on imidazole functionalized silica coated cobalt ferrite nanoparticles was prepared. The synthesized catalyst was characterized by X-ray powder diffraction (XRD), transmission electron microscopy (TEM), vibrating sample magnetometry (VSM), thermogravimetric analysis (TGA), Fourier transform infrared (FT-IR), and inductively coupled plasma atomic emission spectroscopy (ICP-AES). The immobilized phosphotungstic acid was shown to be an efficient heterogeneous catalyst for the synthesis of α-aminophosphonates under solvent-free conditions at room temperature. The catalyst is readily recovered by simple magnetic decantation and can be recycled several times with no significant loss of catalytic activity.

1. Introduction

The choice of an efficient support could significantly improve the activity, selectivity, recycling, and reproducibility of catalyst systems. In recent years, magnetic nanoparticles (MNPs) have emerged as attractive solid supports for immobilization of homogeneous catalysts [1,2]. This is because the magnetic nanoparticles can be well dispersed in the reaction mixtures in the absence of magnetic field providing large surface for readily access of substrate molecules. More importantly, after completing the reactions, the MNPs supported catalysts can be isolated efficiently from the product solution through a simple magnetic separation process thereby eliminating the requirement of catalyst filtration and centrifugation [3,4].

Among the various magnetic nanoparticles, magnetite (Fe_3O_4) is the most widely used magnetic substance for catalysts support [5,6]. However, Fe_3O_4 is fairly reactive to acidic environment and since it contains Fe^{2+}, which is readily oxidized, the MNPs of Fe_3O_4 are vulnerable to lose magnetism. On the contrary, cobalt ferrite ($CoFe_2O_4$) which is a typical ferromagnetic oxide with spinel structure has high thermal stability, moderate magnetization, remarkable chemical stability and mechanical hardness [7,8]. Therefore, cobalt ferrite can show better performance than magnetite as support for homogeneous catalysts. In most cases, the catalytic species cannot be introduced directly on the surface of MNPs supports and modification or functionalization of the MNPs surface is required prior to catalyst immobilization. In a recent review, Basset and co-workers have reported myriad catalytic systems devised by employing some superparamagnetic nanoparticles as a support, and their performance in catalyzing various organic reactions [9].

Polyoxometalates (POMs) and their derivatives have been widely used in organic synthesis and catalytic reactions as acid and oxidation catalysts because of their strong acidity and favourable redox properties [10,11]. Although many procedures have been performed to immobilize polyoxometalates on solid materials, only few reports have recently appeared in the literature about polyoxometalates supported-MNPs. The first example of non-covalent immobilization of POMs on MNPs was reported by Luo and co-workers [12]. These researchers have used Fe_3O_4 MNPs as core and after coating this core with silica, the surface was functionalized with imidazulium group. In the final step, PTA was immobilized on the surface of silica coated MNPs in THF by sonication. The prepared composite was used as efficient acid catalyst for the Friedel–Crafts reaction of indole and chalcones, In another report, oxidation of dibenzothiophene with H_2O_2 was studied by Ding and co-workers using two types nanosized catalysts consisting of phosphotungstic acid ($H_3PW_{12}O_{40}$) supported on surface-modified Fe_3O_4. In this

---

* Corresponding author. Tel.: +98 916 1115451; fax: +98 6113331042.
E-mail address: m_kooti@scu.ac.ir (M. Kooti).

1381-1169/$ – see front matter © 2013 Elsevier B.V. All rights reserved.
http://dx.doi.org/10.1016/j.molcata.2013.02.018

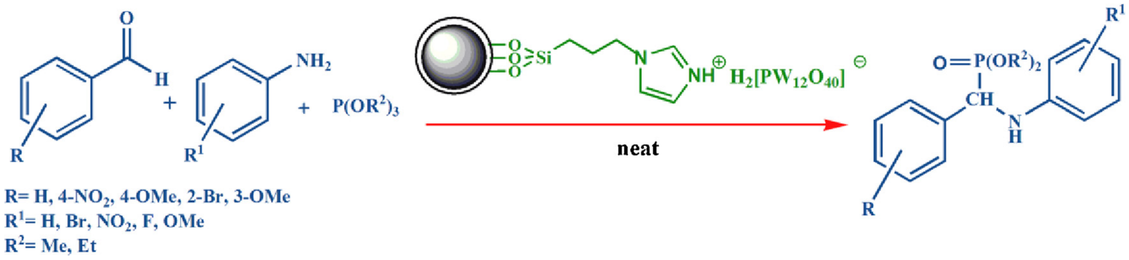

Scheme 1. PTA/Si-imid@ Si-MNPs catalyzed synthesis of α-aminophosphonates.

study high conversions were obtained and the catalysts could be easily separated from the reaction solution by applying an external magnetic field and recycled several times [13]. The oxidation of dibenzothiophene with hydrogen peroxide was also studied by another researcher group using a recyclable amphiphilic catalyst in which phosphotungstic acid was immobilized on surface modified MNPs [14].

In the present work, we designed a methodology for constructing of a magnetically recoverable nanocatalyst in which phosphotungstic acid (PTA) was immobilized on imidazole functionalized silica coated cobalt ferrite nanoparticles. In view of the immense importance of α-aminophosphonates [15–18], the as-synthesized catalyst was utilized for the preparation of these organophosphorous compounds at room temperature under solvent-free conditions (see Scheme 1).

2. Experimental

2.1. General

All chemicals were purchased from Sigma–Aldrich or Merck and used as received. Phosphotungstic acid (PTA) was synthesized according to the literature [19]. X-ray diffraction (XRD) patterns were recorded with a Philips X-ray diffractometer (Model PW1840). FT-IR spectra were obtained using BOMEM MB-Series 1998 FT-IR spectrometer. Magnetic properties of all nanoparticles were measured with a vibrating sample magnetometer (VSM, Meghnatis Daghigh Kavir Company, Iran) at room temperature. The content of tungsten of the PTA/Si-imid@ Si-MNPs catalyst was determined using an ICP-AES instrument (HORIBA Jobin Yvon, Longjumeau Cedex, France). The catalyst sample was first dissolved in concentrated hydrochloric acid and after filtration, the aqueous solution is converted to aerosols via a nebulizer. The aerosols are transported to the inductively coupled plasma with argon flowrate of 12 L/min. NMR spectra were recorded in $CDCl_3$ on a Bruker Advanced DPX 400 MHz spectrometer.

2.2. Synthesis of PTA supported on imidazole functionalized Si-MNPs

Cobalt ferrite MNPs were synthesized using the procedure reported by Maaz et al. [20]. Silica coated $CoFe_2O_4$ nanoparticles (Si-MNPs) were prepared by using a reported sol–gel method [21]. The synthesis of PTA supported on imidazole functionalized Si-MNPs were achieved by using the previously reported method with some modification [22]. In our modified procedure 3-chloromethoxypropylsilane and imidazole in 1:1 molar ratio were reacted first to obtain product 1 (see Scheme 2). This product was then dissolved in ethanol followed by addition of Si-MNPs and the mixture was refluxed for 24 h to give product 3. Finally, PTA/Si-imid@ Si-MNPs composite was obtained by treating of product 3 with PTA in refluxing acetonitrile.

2.3. General procedure of catalytic α-aminophosphonates synthesis

A mixture of an aldehyde (1 mmol), aniline (1 mmol), triethyl phosphate or trimethyl phosphate (1.2 mmol) and PTA/Si-imid@ Si-MNPs catalyst (0.05 g) was stirred for an appropriate time at room temperature. The progress of the reaction was monitored by TLC. At the end of the reaction, CH_3Cl was added to dilute the reaction mixture and the organic layer was simply decanted by means of an external magnet. The isolated solution was purified on a silica-gel plate to obtain pure product. The identities of the products were confirmed by FT-IR and ^1H NMR spectral data.

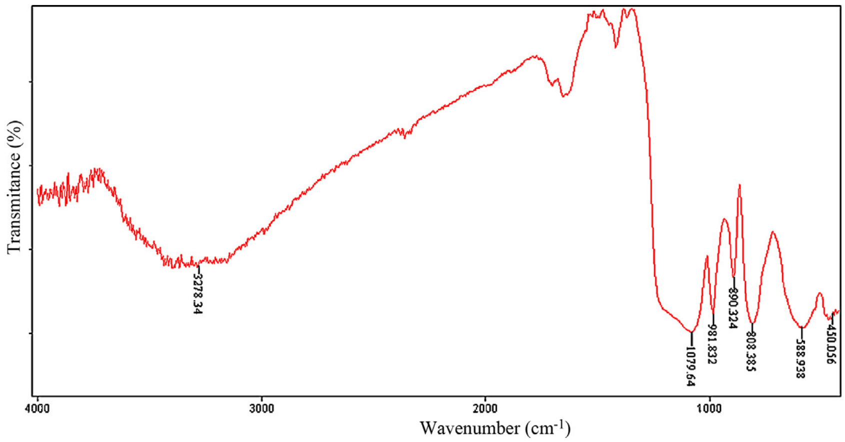

Fig. 1. FT-IR spectrum of PTA/Si-imid@ Si-MNPs.

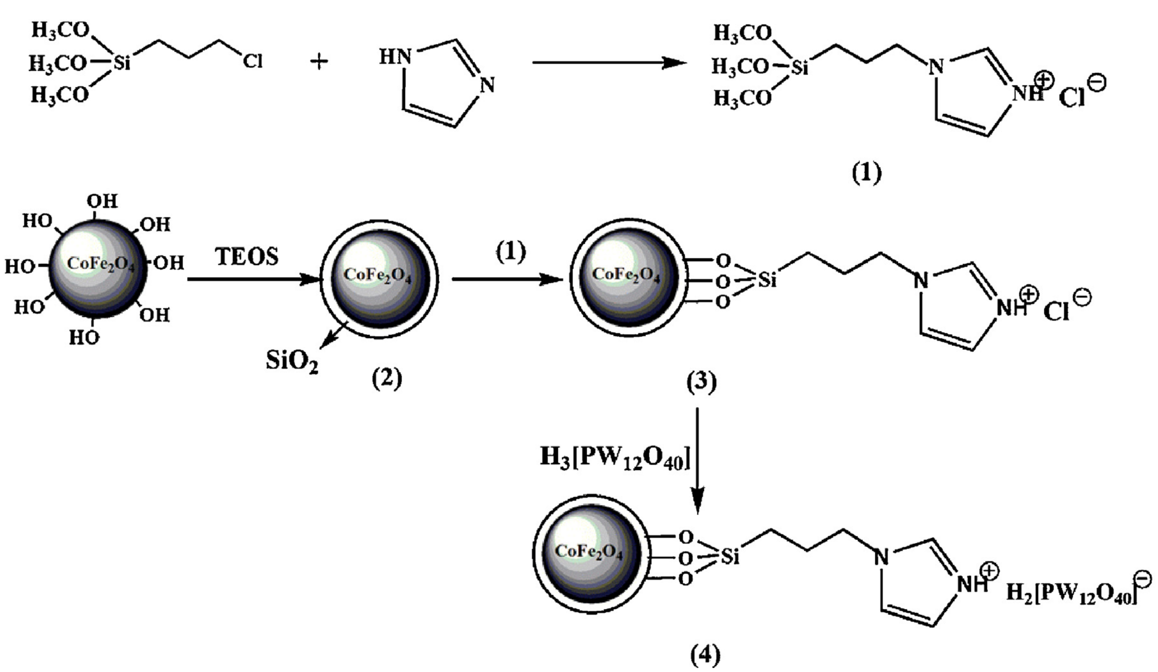

Scheme 2. Schematic representation of the formation of PTA/Si-imid@ Si-MNPs.

3. Results and discussion

3.1. Characterization of PTA/Si-imid@ Si-MNPs

Immobilization of PTA on imidazole functionalized MNPs combines the advantages of ionic liquids with those of heterogeneous catalysts [23]. The PTA moiety in the synthesized catalyst is bonded strongly to Si-imid@ Si-MNPs by means of ionic interaction. The as-synthesized PTA/Si-imid@ Si-MNPs catalyst was characterized by various techniques. The FT-IR spectrum of PTA/Si-imid@ Si-MNPs, shows weak peaks in the range between 1400 and 1630 cm^{-1} assigned to the imidazole ring and two more bands at 890 cm^{-1} and 981 cm^{-1} attributed to the immobilized PTA [24]. In addition, the characteristic peaks of Fe—O at 588 cm^{-1} [25] and Si—O—Si at 1079 cm^{-1} and 808 cm^{-1} [24] were also observed (Fig. 1).

The X-ray diffraction patterns of MNPs, Si-MNPs and PTA/Si-imid@ Si-MNPs are shown in Fig. 2. The peaks are compatible with pure $CoFe_2O_4$ phase (JCPDS PDF #221086), indicating the retention of cubic reverse spinel structure of $CoFe_2O_4$ during coating and functionalization. A weak broad bump appeared in the patterns of Si-MNPs and PTA/Si-imid@ Si-MNPs (Fig. 2b and c), at $2\theta = 18–28°$, could be assigned to an amorphous silica phase in the shell of $CoFe_2O_4$. There are, however, no characteristic peaks of PTA in the XRD pattern of PTA/Si-imid@ Si-MNPs. This indicates that PTA species are well-dispersed on the surface of Si-imid@ Si-MNPs and probably there is no crystalline phase of this heteropoly acid to be detected by XRD analysis [26,27]. The crystallite sizes of cobalt ferrite MNPs, Si-MNPs and PTA/Si-imid@ Si-MNPs estimated using the well-known Scherer formula [28] were found to be 25.5 nm, 34.7 nm and 34.9 nm respectively. The growth of magnetic nanoparticles on coating with silica was also occurred in the previously reported composites [29–31]. No explanation was given for this observation in any of the reported works; however, this increase might be due to the strong interaction of Si—O groups with the metal cations on the surface of the MNPs which in turn brings the crystallites closer to each other and fuse them to somewhat larger particles.

The TEM image of PTA/Si-imid@ Si-MNPs is presented in Fig. 3, showing that most of the particles have quasi-spherical shape. The

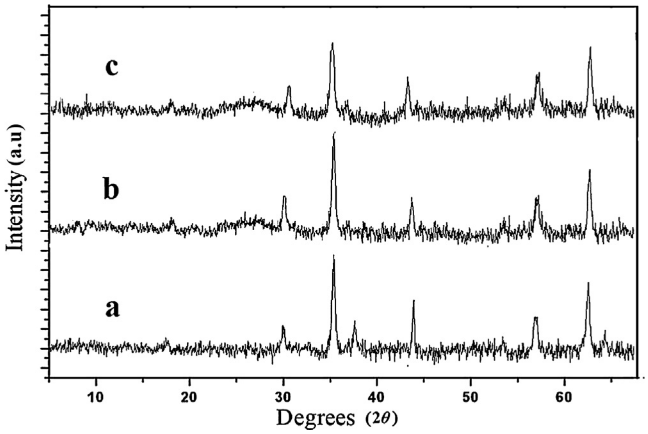

Fig. 2. XRD patterns of (a) MNPs, (b) Si-MNPs and (c) PTA/Si-imid@ Si-MNPs.

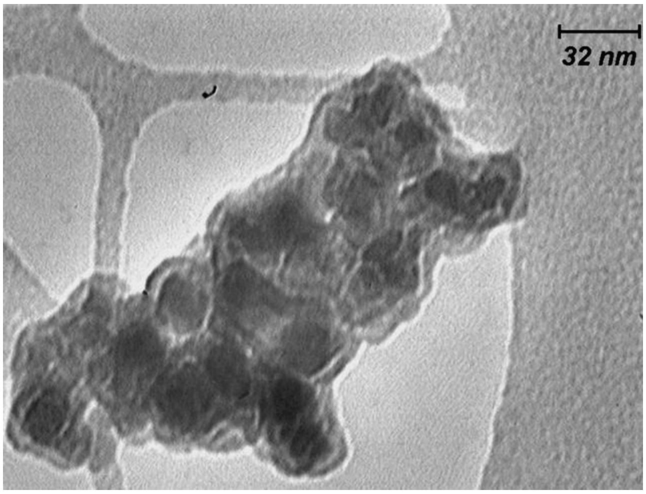

Fig. 3. TEM image of PTA/Si-imid@ Si-MNPs.

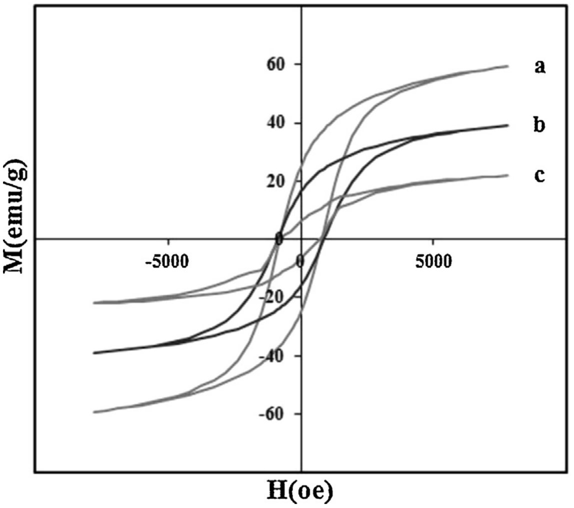

Fig. 4. Hysteresis loops of (a) MNPs, (b) Si-MNPs and (c) PTA/Si-imid@ Si-MNPs.

average size of these nanoparticles is in the range of 20–30 nm which shows a close agreement with the values calculated by XRD data. Interestingly, the magnetic core is visible as a dark spot inside the bright spherical SiO_2 thin shell in the TEM image of PTA/Si-imid@ Si-MNPs sample.

Magnetic measurements for MNPs, Si-MNPs and PTA/Si-imid@ Si-MNPs were performed using a vibrating sample magnetometer (VSM) with a peak field of 8 kOe and their hysteresis curves are presented in Fig. 4. It could be seen from the loops in Fig. 4 that saturation magnetization (M_S) of MNPs, Si-MNPs and PTA/Si-imid@ Si-MNPs are 59.42, 38.93 and 21.84 emu g^{-1} respectively. The decrease in mass saturation magnetization may be ascribed to the contribution of the non-magnetic silica shell and functionalized groups. Interestingly, although the M_S values of the silica coated and functionalized MNPs samples have remarkably decreased, they still could be efficiently separated from solution with a permanent magnet.

There are two weight loss steps in TGA curve of PTA/Si-imid@ Si-MNP catalyst (Fig. 5). The first mass loss of 1.7% (between 60 and 218 °C) may be due to removal of surface adsorbed water of the catalyst. The loss of weight at temperatures higher than 218 °C can be ascribed to the decomposition of Si-imid groups. The TGA analysis of the as-prepared catalyst showed that the loading of immidazolium moiety about 0.36 mmol/g. Moreover, the tungsten content of the catalyst, as determined by ICP-AES, was 0.98 mmol/g. This is another proof for the fact that PTA was immobilized onto the imidazole functionalized silica coated $CoFe_2O_4$.

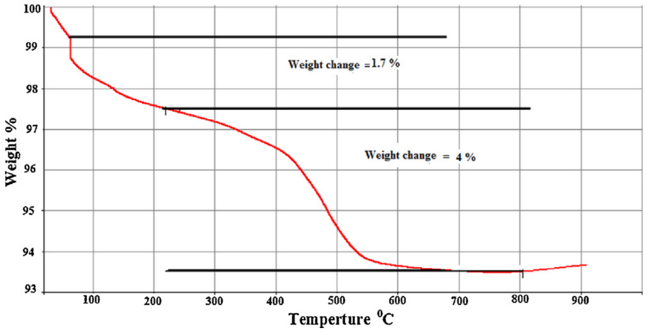

Fig. 5. TGA of PTA/Si-imid@ Si-MNPs.

Table 1

Effect of various catalysts and solvents on the synthesis of α-aminophosphonates.

Entry	Catalyst	Solvent	Time (min)	Yield[b] (%)
1	PTA/Si-imid@SiMNPs	CH_3CN	20	80
2	PTA/Si-imid@SiMNPs	CH_2Cl_2	30	85
3	PTA/Si-imid@SiMNPs	EtOH	45	75
4	PTA/Si-imid@SiMNPs	$(CH_3)_2CO$	45	60
5	SiMNPs	Neat	120	30
6	Si-imid@SiMNPs	Neat	120	74
7	PTA/Si-imid@SiMNPs	Neat	15	95

[a] All reaction conditions: benzaldehyde (1 mmol), aniline (1 mmol), $P(OEt)_3$ (1.2 mmol), catalyst (0.05 g) at room temperature.

[b] Isolated yield.

3.2. α-Aminophosphonates synthesis

In order to optimize the reaction conditions of α-aminophosphonates synthesis, various experiments were carried out at room temperature using benzaldehyde, aniline and triethylphosphate substrates in the presence of PTA/Si-imid@ Si-MNPs as catalyst. Firstly, we screened different solvents such as CH_3CN, acetone, CH_2Cl_2, and EtOH to find out the effect of solvent on the progress of reaction. The results are given in Table 1. When this reaction was carried out under solvent-free conditions, however, much better results were obtained (see Table 1).

Secondly, to see the effectiveness of PTA species on this catalysis reaction, we have also examined Si-MNPs and Si-imid@ Si-MNPs in addition to PTA/Si-imid@ Si-MNPs as catalysts in separate experiments. As seen in Table 1, PTA/Si-imid@ Si-MNPs showed the best catalytic activity for the α-aminophosphonates synthesis.

In order to explore the scope and the limitations of this novel catalytic method of α-aminophosphonates synthesis, we investigated various aromatic aldehydes and amines containing either electron withdrawing or electron donating functional groups with $P(OEt)_3$ and $P(OMe)_3$ under solvent-free conditions. The given results in

Table 2

Synthesis of diversified α-aminophosphonates in the presence of PTA/Si-imid@ Si-MNPs.[a]

Entry	Aldehyde	R^1 (amine)	R^2	Time (min)	Yield[b] (%)
1	R=H	H	Me	15	94
2	R=H	H	Et	15	95
3	R=H	2-Br	Et	20	97
4	R=H	4-F	Et	35	86
5	R=H	4-OMe	Et	30	88
6	R=H	$4\text{-}NO_2$	Me	30	91
7	R=3-OMe	H	Me	20	88
8	R=3-OMe	H	Et	20	91
9	R=3-OMe	4-Br	Et	30	90
10	R=3-OMe	4-F	Et	25	91
11	R=3-OMe	4-OMe	Et	20	92
12	R=2-Br	H	Me	20	94
13	R=2-Br	H	Et	30	91
14	R=2-Br	4-Br	Et	30	89
15	R=2-Br	4-F	Et	20	94
16	R=2-Br	4-OMe	Et	20	97
17	R=4-OMe	H	Me	35	92
18	R=4-OMe	H	Et	20	94
19	R=4-OMe	4-Br	Et	25	90
20	R=4-OMe	4-F	Et	20	87
21	R=4-OMe	2-Br	Et	20	92
22	$R=4\text{-}NO_2$	H	Me	15	97
23	$R=4\text{-}NO_2$	H	Et	15	96
24	$R=4\text{-}NO_2$	2-Aminopyridine	Me	25	78
25	Furfural	H	Me	30	81
26	Furfural	2-Aminopyridine	Me	40	68

[a] All reaction condition: aldehydes (1 mmol), amine (1 mmol), $P(OMe)_3/P(OEt)_3$ (1.2 mmol) and 0.05 g of PTA/Si-imid@ Si-MNPs at room temperature.

[b] Isolated yields.

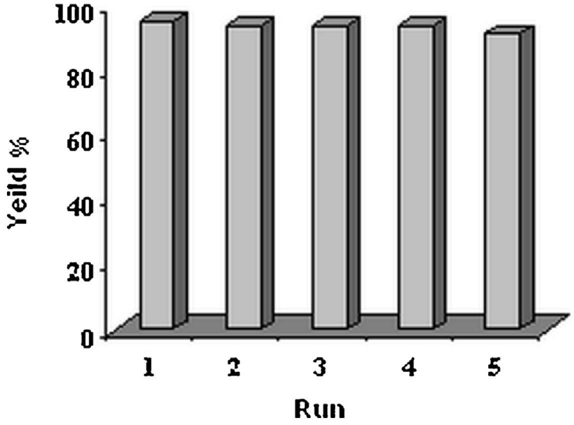

Fig. 6. Catalyst recycling experiments for α-aminophosphonates synthesis.

Table 2 show that this one pot, three component condensations completed within 15–40 min, with good isolated yields. The lower yields obtained for furfural and 2-amino pyridine are probably due to the lower reactivity of the heterocyclic substrates.

Many methods have been so far developed for the synthesis of α-aminophosphonates [32–35]. However, in spite of their potential utility, most of these synthetic routes still have certain limitations such as use of solvents and toxic catalyst, longer reaction time, elevated temperature, and comparative more tedious work up purification procedures, thereby restrict their applications. Our catalysis synthesis of α-aminophosphonates can eliminate almost all these drawbacks since high yield of α-aminophosphonates was obtained in a short reaction time at room temperature under solventless condition. Most importantly, the catalyst can be readily separated from the reaction product by means of magnetic decantation and used for several time with no noticeable loss of its activity.

3.3. *Catalyst recycling*

To evaluate the stability and level of reusability of the catalyst, we conducted experiments of α-aminophosphonates synthesis using the recycled PTA/Si-imid@ Si-MNPs catalyst. After the completion of the first reaction, the catalyst was washed with CH_3Cl and the solution was removed by magnetic decantation. The left used catalyst was washed with methanol and $CHCl_3$ and dried. A new reaction was then conducted with fresh reactants under similar conditions. It was found that the developed catalyst could be used at least five times without any change in reactivity (see Fig. 6). ICP-AES analysis has shown that slight leaching of the catalyst from support (0.92 wt%) occurred only in the first run and no leaching was observed in the next runs. Moreover, the FT-IR spectrum of the recovered catalyst showed no change after using it for five times. This indicates that no significant leaching of the PTA species occurred from support on using and reusing the catalyst.

4. Conclusions

In summary, we have successfully developed a novel type of non-covalently immobilized $H_3PW_{12}O_{40}$ catalyst using surface-modified $CoFe_2O_4$ magnetic nanoparticles as support. The synthesized catalyst was confirmed by XRD, FT-IR, TGA, TEM, ICP-AES, and VSM techniques. The immobilized phosphotungstic acid was shown to be an efficient heterogeneous catalyst for synthesis of α-aminophosphonates under solvent-free conditions at room temperature. Moreover, the immobilized PTA catalyst could be easily recovered by simple magnetic decantation and reused at least five times without significant loss of activity.

Acknowledgment

The authors wish to acknowledge the support of this work by the Research Council of Shahid Chamran University, Ahvaz, Iran.

References

[1] C.W. Lim, I.S. Lee, Nano Today 5 (2010) 412.
[2] S. Shylesh, V. Schunemann, W.R. Thiel, Angew. Chem. Int. Ed. 49 (2010) 3428.
[3] P. Riente, C. Mendoza, M.A. Pericas, J. Mater. Chem. 21 (2011) 7350.
[4] R. Abu-Rezig, H. Alper, D. Wang, M.L. Post, J. Am. Chem. Soc. 128 (2006) 5279.
[5] Y. Qiang, J. Antony, J. Nutting, D. Sikes, D. Meyer, J. Nanopart. Res. 8 (2006) 489.
[6] A. Kong, P. Wang, H. Zhang, F. Yang, S.P. Huang, Y. Shan, Appl. Catal., A 417 (2012) 183.
[7] R.S. Turtelli, G.V. Duong, J. Magn. Magn. Mater. 320 (2008) 339.
[8] C. Cannas, A. Ardu, A. Musinu, D. Peddis, G. Piccaluga, Chem. Mater. 20 (2008) 6364.
[9] V. Polshettiwar, R. Luque, A. Fihri, H. Zhu, M. Bouhrara, J.M. Basset, Chem. Rev. 111 (2011) 3036.
[10] N. Mizuno, M. Misono, Chem. Rev. 98 (1998) 199.
[11] M.T. Pope, A. Muller, Angew. Chem. Int. Ed. 30 (1991) 34.
[12] X. Zheng, L. Zhang, J. Li, S. Luo, J.P. Cheng, Chem. Commun. 47 (2011) 12325.
[13] Z. Zhang, F. Zhang, Q. Zhu, W. Zhao, B. Ma, Y. Ding, J. Colloid Interface Sci. 360 (2011) 189.
[14] X. Cui, D. Yao, H. Li, J. Yang, D. Hu, J. Hazard. Mater. 205 (2012) 17.
[15] F.R. Atherton, C.H. Hassall, R.W. Lambert, J. Med. Chem. 29 (1986) 29.
[16] X. Rao, Z. Song, L. He, Heteroat. Chem. 19 (2008) 512.
[17] I. Kraicheva, A. Bogomilova, I. Tsacheva, G. Momekov, K. Troev, Eur. J. Med. Chem. 44 (2009) 3363.
[18] P. Kafarski, B. Lejczak, Phosphorus Sulfur Silicon Relat. Elem. 63 (1991) 193.
[19] J.C. Bailar, Inorg. Synth. 1 (1939) 132.
[20] K. Maaz, A. Mumtaz, S.K. Hasanain, A. Ceylan, J. Magn. Magn. Mater. 308 (2007) 289.
[21] Y.H. Deng, C.C. Wang, J.H. Hu, W.L. Yang, S.K. Fu, Colloids Surf., A 262 (2005) 87.
[22] L.T.A. Sofia, A. Krishnan, M. Sankar, N.K. Kala Raj, P. Manikandan, P.R. Rajamohanan, T.G. Ajithkumar, J. Phys. Chem. C 113 (2009) 21114.
[23] C.P. Mehnert, J. Chem. Eur. 11 (2005) 50.
[24] H. Ono, T. Katsumata, Appl. Phys. Lett. 78 (2001) 1832.
[25] M. Ma, Y. Zhang, W. Yu, H.Y. Shen, H. Zhang, N. Gu, Colloids Surf., A 212 (2003) 219.
[26] Y. He, C.S. Woo, H.G. Kim, H.I. Lee, Appl. Catal., A 281 (2005) 167.
[27] A.G. Siahkali, A. Philippou, J. Dwyer, M.W. Anderson, Appl. Catal., A 192 (2000) 57.
[28] B.D. Cullity, Elements of X-ray Diffraction, Addison-Wesley, London, 1978.
[29] Q. Xiao, C. Xiao, Nanoscale Res. Lett. 4 (2009) 1078.
[30] S. Zhang, D. Dong, Y. Sui, Z. Liu, H. Wang, Z. Qian, W. Su, J. Alloys Compd. 415 (2006) 257.
[31] S. Modak, S. Karan, S.K. Roy, S. Mukherjee, D. Das, P.K. Chakrabarti, J. Magn. Magn. Mater. 321 (2009) 169.
[32] M. Tajbakhsh, A. Heydari, H. Alinezhad, M. Ghanei, S. Khaksar, Synthesis (2008) 352.
[33] Z. Rezaei, H. Firouzabadi, N. Iranpoor, A. Ghaderi, M.R. Jafari, A.A. Jafari, H.R. Zare, Eur. J. Med. Chem. 44 (2009) 4266.
[34] M. Ordonez, H. Rojas-Cabrera, C. Cativiela, Tetrahedron 65 (2009) 17.
[35] A. Heydari, H. Hamadi, M. Pourayoubi, Catal. Commun. 8 (2007) 1224.